# Unimolecular Nanocontainers Prepared by ROP and Subsequent ATRP from Hydroxypropylcellulose

**Emma Östmark, Daniel Nyström, and Eva Malmström***

*Department of Fibre and Polymer Technology, KTH School of Chemical Science and Engineering, Royal Institute of Technology, Teknikringen 56-58, SE-100 44 Stockholm, Sweden*

*Received December 3, 2007; Revised Manuscript Received March 17, 2008*

ABSTRACT: Hydroxypropylcellulose (HPC) is used as a macroinitiator for ring-opening polymerization of ε-caprolactone for the synthesis of a high molecular weight comb polymer consisting of a cellulose backbone and PCL grafts. The PCL end groups are converted into initiating sites for ATRP and chain extension of the PCL block is performed through grafting of *tert*-butyl acrylate to different lengths. The comb block copolymers are thereafter converted to amphiphilic polymers through deprotection of the *tert*-butyl group by acidic treatment, resulting in PCL-*block*-PAA grafts. These block copolymers are suspended in water and cross-linked using a water-soluble diamine to different attempted cross-link densities. Initial studies of the solubilization and encapsulation capacities of the amphiphilic polymers are performed using the hydrophobic model compound pyrene.

## Introduction

Amphiphilic block copolymers are of wide interest due to their ability to self-assemble into micelles possessing a nanoscale, well-defined structure. Wooley and co-workers pioneered this field with the development of shell cross-linked knedels (SCKs),[1] robust nanoparticles with controllable size and interior- and surface function, and since then other groups have followed.[2] These nanoparticles are self-assembled from well-defined amphiphilic block copolymers and subsequently cross-linked to stabilize their shape and size. Removal of the core domain has been performed to prepare hollow nanoparticles (nanocages)[3,4] that are potential carriers of guest molecules thanks to their high loading capacity.

The interest in using unimolecular micelles, a single molecule with a hydrophobic and hydrophilic part, is steadily growing. The term unimolecular micelle was coined by Newkome and co-workers and denoted a system with a water-soluble, end-group-functionalized dendrimer, capable of encapsulating guest molecules due to internal hydrophobic voids.[5] Since then, a range of amphiphilic dendrimers have showed encapsulation and solubilization capacity, in both water[6] and organic media.[7] The benefits of using unimolecular micelles compared to traditional ones are several: their enhanced thermal stability, their static nature, and the lack of concentration dependence upon formation. The surface properties of these unimolecular micelles, and the size of the core domain, have recently been modified by grafting, employing "living"/controlled polymerization techniques of suitable monomers.[8,9] The encapsulation efficiency of block copolymer-based unimolecular micelles has also been studied.[10−13]

The interest in using water-soluble nanocarriers stems from their possible applications in biomedicine.[14] However, the sizes of the nanoparticles are often small, which give them too short retention time in the body and lower loading capacities.[14,15] The need for larger particles, still on the nanoscale, with properties such as water suspendability, encapsulation efficiency, and biocompatibility is urgent.

Cellulose is the most abundant natural polymer and benefits from being a renewable and biodegradable material with high mechanical strength, available at a low cost. Chemical modification of cellulose to suit certain applications, such as graft polymerization from cellulose, has been performed since the beginning of the past century. The traditional methods usually results in uneven grafting of the cellulose and insoluble molecules. However, direct tailoring of the properties was not possible until cellulose was subjected to the "living"/controlled polymerization techniques, since a predetermined degree of polymerization (DP) and end-group control are the possible outcomes of these techniques. Atom transfer radical polymerization (ATRP) is a controlled polymerization technique that is extensively used owing to its versatility and compatibility with a range of monomers.[16−18] Initially, filter paper was, due to its high cellulose content, the most suitable candidate for the development of ATRP from cellulose,[19−24] and the success of this graft modification subsequently led to ATRP from cellulose in solution.[25−30] However, ring-opening polymerization (ROP) has also proven to be a versatile controlled polymerization technique useful for grafting. Cellulose, both as solid substrate and as soluble polymer, has been thoroughly studied as macroinitiator for ROP of ε-caprolactone and L-lactide.[31−36] The resulting copolymers are of interest due to their biodegradability and the possibility to tailor their degree of crystallinity.[31,35] Other controlled polymerization techniques such as nitroxide-mediated polymerization[37] (NMP) and reversible addition−fragmentation chain transfer polymerization[38−41] (RAFT) have also been used for grafting from cellulose.

In the present paper, hydroxypropylcellulose (HPC) is used as a backbone for the production of unimolecular nanocontainers. ROP of ε-caprolactone from HPC provides a biocompatible, high molecular weight comb polymer. The grafts of this comb polymer are chain extended via ATRP and postfunctionalized to yield an amphiphilic comb block copolymer with a poly(acrylic acid) corona, thus accomplishing a water suspendable polymer. These amphiphilic polymers are shell cross-linked in dilute water solution to produce nanoparticles with hydrogel-like shell. The nanoparticle encapsulation ability of the model hydrophobic compound pyrene is subjected to an initial investigation.

## Experimental Section

**Materials.** Hydroxypropylcellulose (HPC; $M_n = 10\,000$ g mol$^{-1}$, $M_w = 80\,000$ g mol$^{-1}$ according to manufacturer (Aldrich); $M_n = 25\,200$ g mol$^{-1}$, $M_w = 63\,600$ g mol$^{-1}$ obtained using SEC with

* To whom correspondence should be addressed: Tel +46 8 7908273, Fax +46 8 7908283, e-mail mave@polymer.kth.se.

10.1021/ma702681u CCC: $40.75 
Published on Web 05/17/2008

**Scheme 1. Ring-Opening Polymerization of ε-Caprolactone Initiated by Hydroxypropylcellulose**

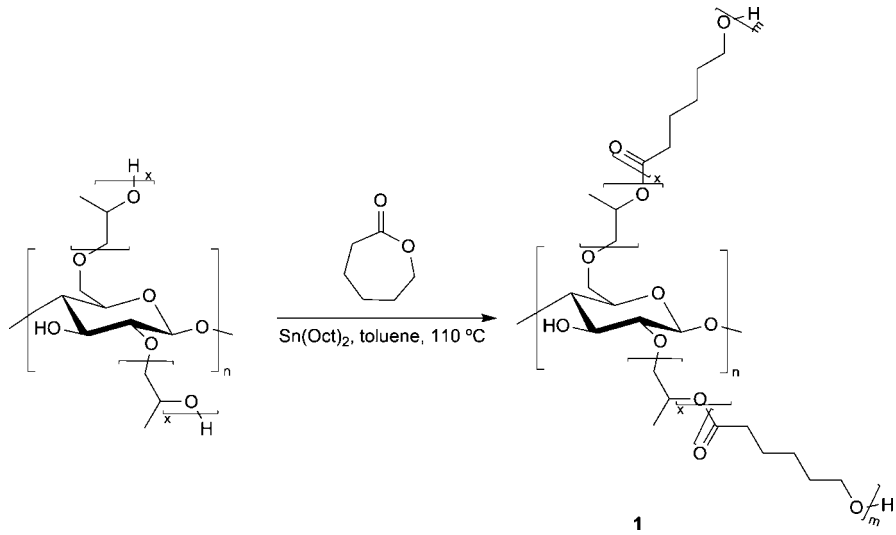


THF as mobile phase, molar substitution of propoxy groups ($MS_{HP}$) 2.9 determined using $^1$H NMR)[30] was purchased from Aldrich and was dried 24 h in a vacuum oven at 50 °C before use. 2-Bromoisobutyryl bromide (98%), *N,N,N′,N″,N″*-pentamethyldiethylenetriamine (PMDETA) (99%), copper(I) bromide (98%), copper(II) bromide (99%), ε-caprolactone (99%), *tert*-butyl acrylate (98%, passed through a column containing neutral aluminum oxide (Merck) before use), stannous 2-ethylhexanoate (∼95%), and THF (spectrophotometric grade, ≥99.5%) were purchased from Aldrich. 4-(Dimethylamino)pyridine (DMAP, 99%), triethylamine (TEA), and trifluoroacetic acid (TFA, 99%) were used as received from Acros. Pyrene was purchased from Eastman-Kodak.

**Instrumentation.** *Nuclear Magnetic Resonance.* $^1$H and $^{13}$C NMR spectra were recorded on a Bruker Avance 400 MHz NMR instrument using $CDCl_3$, THF-$d_8$, and $D_2O$. The solvent signals were used as internal standards.

*Fourier Transform Infrared Spectroscopy.* The absorption spectra from the samples were collected by employing a Perkin-Elmer Spectrum 2000 FT-IR equipped with a MKII Golden Gate, Single Reflection ATR System from Specac Ltd., London, UK. The ATR crystal was a MKII heated Diamond 45° ATR top plate. Sixteen scans were recorded for each spectrum.

*Size Exclusion Chromatography.* SEC using THF (1.0 mL min$^{-1}$) as the mobile phase was performed at 35 °C using a Viscotek TDA model 301 equipped with two $GMH_{HR}$-M columns with TSK-gel (mixed bed, MW resolving range: 300−100 000) from Tosoh Biosep, a VE 5200 GPC autosampler, a VE 1121 GPC solvent pump, and a VE 5710 GPC degasser (all from Viscotek Corp.). A calibration method was created using narrow linear polystyrenes standards. Corrections for the flow rate fluctuations were made using toluene as an internal standard. Viscotek OmniSEC version 4.0 software was used to process data. The samples were heated to 60 °C during 2 h and filtered through 0.45 μm filters twice, prior to analysis.

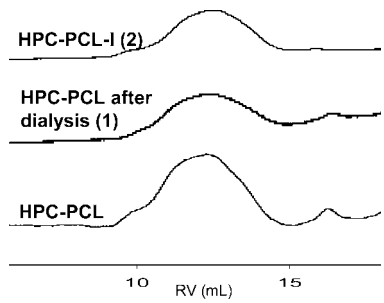


**Figure 1.** SEC traces of HPC-PCL (lower), HPC-PCL after dialysis (middle), and HPC-PCL-I (upper).

**Table 1. Molecular Weight Averages and Molecular Weight Distribution for Hydroxypropylcellulose, Poly(ε-caprolactone)-Grafted Hydroxypropylcellulose (HPC-PCL), and Initiator-Modified HPC-PCL (HPC-PCL-I) Obtained Using SEC in THF**

| sample no. | sample | $M_n$ (g mol$^{-1}$) | $M_w$ (g mol$^{-1}$) | PDI |
|---|---|---|---|---|
| | HPC | 25 200 | 63 600 | 2.5 |
| **1** | HPC-PCL | 158 700 | 365 300 | 2.3 |
| **2** | HPC-PCL-I | 142 400 | 348 000 | 2.4 |

*Atomic Force Microscopy.* AFM samples were prepared through spin-casting (3500 rpm, 90 s) solution of polymer samples (0.01−1.0 mg mL$^{-1}$) in THF or drop-casting from water and dried 30 min in a vacuum oven at 50 °C, onto freshly cleaved mica. AFM was performed using a Nanoscope III-a system (Digital Instruments, Santa Barbara, CA) equipped with a J-type- or EV-type vertical engage piezoelectric scanner operating in tapping mode in air. Silicon AFM probes from Veeco were used throughout the study ($l$ = 115−135 μm, force constant 20−80 N/m, resonance frequency 267−348 kHz).

*UV Absorbance.* A WPA Lightwave UV/vis diode array spectrophotometer was operated at 25 °C. Quartz cuvettes ($l$ = 10 mm) were used to measure the UV/vis absorption in the range 200−825 nm of samples in deionzed water or THF.

*Dynamic Light Scattering.* The zeta average was determined using a Malvern ZEN 3600 Zetasizer Nano ZS instrument operating a 632.8 nm. The scattering was recorded at 173° angle at 25 °C in THF (spectrophotometric grade) or deionized water assuming a polymer RI of 1.59. Data collection was performed for 1 h. Only measurements which showed a low cumulant fit error were used. Prior to analysis, all samples were centrifuged (3500 rpm, 4 min). In addition, the samples prepared in THF were heated to 60 °C for 2 h before centrifugation and filtered through 0.45 μm Teflon filters twice. The amphiphilic polymers (non-cross-linked) were filtered through 0.45 μm sulfone filters.

*Thermogravimetric Analysis (TGA).* TGA was performed on a Mettler Toledo TGA/SDTA851 TGA module and evaluated using STARe software, version 8.10. Heating was performed at 10 °C min$^{-1}$ with an $N_2$ flow of 30 mL min$^{-1}$.

*Differential Scanning Calorimetry.* DSC thermograms were collected using a Mettler Toledo DSC820 using a heating/cooling rate of 10 °C min$^{-1}$ under a $N_2$ atmosphere. Values from the second heating scan were used. STARe software, version 8.10, was used to evaluate data.

**Syntheses.** *Ring-Opening Polymerization of ε-Caprolactone from Hydroxypropylcellulose (***1***).* Hydroxypropylcellulose (HPC; 2.58 g, ca. 15.2 mmol of OH groups) was allowed to dissolve in

**Table 2. Results of ATRP of t-BA from Initiator-Modified HPC-PCL (HPC-PCL-I)**

| | | | SEC[a] | | | $^1$H NMR | | DLS[c] | |
|---|---|---|---|---|---|---|---|---|---|
| sample no. | sample | pol time t-BA (h) | $M_n$ (g mol$^{-1}$) | $M_w$ (g mol$^{-1}$) | PDI | $M_n$[b] (g mol$^{-1}$) | DP[b] | *Z*-average (nm) | PDI[d] |
| **1** | HPC-PCL | | 158 700 | 365 300 | 2.3 | | | 67.6 | 0.53 |
| **2** | HPC-PCL-I | | 142 400 | 348 000 | 2.4 | | | 58.8 | 0.40 |
| **3** | HPC-PCL-PtBA | 1 | 166 700 | 314 300 | 1.9 | 1 900 | 15 | 73.2 | 0.44 |
| **4** | HPC-PCL-PtBA | 2 | | | | 3 200 | 25 | 67.6 | 0.43 |
| **5** | HPC-PCL-PtBA | 5 | | | | 17 100 | 133 | 69.6 | 0.24 |
| **6** | HPC-PCL-PtBA | 14 | | | | 34 100 | 266 | 86.3 | 0.19 |
| **7** | HPC-PCL-PtBA | 17 | | | | 66 400 | 518 | 90.2 | 0.19 |

[a] Obtained by using SEC in THF, 1.0 mL min1, calibrated using linear polystyrene standards. [b] This refers to the $M_n$ and DP of the PtBA-block. The DP of the PCL block is held constant to 11 units. [c] The DLS data were obtained in THF. [d] PDI for cumulative light scattering (0−1). Broad distributions show a PDI close to 1 and the more narrow the lower the PDI.

ε-caprolactone (CL; 16.92 mL, 17.43 g, 15.20 mmol) and toluene (60 mL, 70 g) for 24 h at ambient temperature. When the reaction mixture was completely dissolved, the flask was evacuated and back-filled with Ar gas one time. Stannous 2-ethylhexanoate (2 wt % of monomer, 0.29 g, 0.72 mmol) was added, and the flask was evacuated and back-filled with Ar gas additionally three times and immersed into an oil bath preset to 110 °C. The reaction was allowed to proceed for 2.5 h until the stir bar was unable to move; the rubber septum was removed, and a sample for conversion measurement was withdrawn (84% monomer conversion). The viscous liquid was diluted with THF (ca. 300 mL) and precipitated into methanol. After filtration the product was dried under vacuum at 50 °C, yielding 13.9 g of polymer. The polymer was dissolved in THF and dialyzed (MWCO 6000−8000 Da) against THF for 3 days. The dialyzed polymer was precipitated in MeOH, filtered, and dried under vacuum. The final yield was 12.4 g of HPC-PCL. The maximum weight fraction of HPC in HPC-PCL is calculated to 21% (input mass HPC/resulting HPC-PCL mass = 2.58/12.4 = 20.8%). $^1$H NMR ($CDCl_3$): $\delta$ 1.12 (s, −CH(C$H_3$)OH or −CH(C$H_3$)OCH$_2$−), 1.21 (s, −CH(C$H_3$)OCO−), 1.37 (s, 22.2 H−OCO(CH$_2$)$_2$C$H_2$(CH$_2$)$_2$−), 1.58−1.71 (m, 41.9 H, −OCO-(CH$_2$)$_3$C$H_2$CH$_2$− and −OCOCH$_2$C$H_2$(CH$_2$)$_3$−), 2.30 (t, 21.2 H, −OCOC$H_2$(CH$_2$)$_4$−), 3.64 (t, 2 H, −OCO(CH$_2$)$_4$C$H_2$OH), 4.05 (t, 21.0 H, −OCO(CH$_2$)$_4$C$H_2$OCO−), 5.00 ppm (br, 0.9 H, −C$H$(CH$_3$)OCO−). FT-IR: 3448, 2942, 2866, 1721, 1470, 1417, 1397, 1365, 1298, 1165, 1090, 1046, 961, 935, 840, 732 cm$^{-1}$. $T_m$ = 41 °C.

*Synthesis of ATRP Macroinitiator HPC-PCL-I from HPC-PCL (**2**).* Hydroxypropylcellulose-*g*-poly(caprolactone) (HPC-PCL, **1**, 1.00 g, ca. 1.23 mmol of OH groups) was allowed to dissolve at 60 °C in dry THF (150 mL) overnight. The solution was cooled down to ambient temperature, and triethylamine (TEA, 0.26 mL, 1.84 mmol) and a catalytic amount of 4-(dimethylamino)pyridine (DMAP) were added. 2-Bromoisobutyryl bromide (1.14 mL, 9.24 mmol) in THF (20 mL) was added dropwise under cooling on an ice/water bath, and a white precipitate of the triethylammonium salt was formed. The reaction was allowed to reach completion for 2 h, and the salt was filtered off. The crude product was precipitated in methanol, isolated, and dried under vacuum. $^1$H NMR ($CDCl_3$): $\delta$ 1.12 (s, −CH(C$H_3$)OH or −CH(C$H_3$)OCH$_2$−), 1.21 (s, −CH(C$H_3$)OCO−), 1.38 (s, 23.3 H, −OCO(CH$_2$)$_2$C$H_2$(CH$_2$)$_2$−), 1.58−1.71 (m, 47.2 H, −OCO(CH$_2$)$_3$C$H_2$CH$_2$− and −OCOCH$_2$-C$H_2$(CH$_2$)$_3$−), 1.92 (s, 6.1 H, −COC(C$H_3$)$_2$Br), 2.30 (t, 22.8 H, −OCOC$H_2$(CH$_2$)$_4$−), 4.06 (t, 21.2 H, −OCO(CH$_2$)$_4$C$H_2$OCO−), 4.17 (t, 2.0 H, −OCO(CH$_2$)$_4$C$H_2$OCOC(C$H_3$)$_2$Br), 5.00 ppm (br, 0.9 H, −C$H$(CH$_3$)OCO−). FT-IR: 3443, 2942, 2868, 1721, 1463, 1417, 1394, 1367, 1293, 1239, 1162, 1106, 1067, 1049, 963, 841, 734, 630 cm$^{-1}$. $T_m$ = 33 °C.

*General Procedure for ATRP of tert-Butyl Acrylate from HPC-PCL-I.* To a flask containing *tert*-butyl acrylate (t-BA; 6.00 g, 46.81 mmol), toluene (6.00 g, 50 wt %), and *N,N,N′,N″,N‴*-pentamethyldiethylenetriamine (PMDETA; 81 mg, 0.47 mmol) was added HPC-PCL-I (**2**, 100 mg) and was allowed to dissolve at 70 °C for 15 min. The flask was withdrawn from the oil bath; Cu(I)Br (54 mg, 0.38 mmol) and Cu(II)Br$_2$ (21 mg, 94 μmol) were added, and the flask was sealed with a rubber septum. The flask was evacuated and back-filled with Ar gas three times and thereafter immersed into an oil bath preset to 70 °C. The polymerizations were stopped at different times, according to Table 2. The samples were precipitated in MeOH/water (9/1), filtered, and dried under vacuum. Sample **3** was terminated after 1 h. $^1$H NMR ($CDCl_3$): $\delta$1.13 (s, −CH(C$H_3$)OH or −CH(C$H_3$)OCH$_2$−), 1.25 (s, −CH-(C$H_3$)OCO−), 1.38 (s, 24.1 H, −OCO(CH$_2$)$_2$C$H_2$(CH$_2$)$_2$−), 1.44 (s, 133.2 H, −C(C$H_3$)$_3$), 1.58−1.71 (m, 45.5 H, −OCO-(CH$_2$)$_3$C$H_2$CH$_2$− and −OCOCH$_2$C$H_2$(CH$_2$)$_3$−), 1.80 (br, 3.59 H, 2 −C$H_2$(CHOOC(CH$_3$)$_3$)), 2.15−2.30 (br, −CH$_2$(C$H$OOC-(CH$_3$)$_3$)), 2.31 (t, −OCOC$H_2$(CH$_2$)$_4$−)) 4.06 (t, 22.2 H, −OCO(CH$_2$)$_4$C$H_2$OCO−), 5.00 ppm (br, 0.8 H, −C$H$-(CH$_3$)OCO−). FT-IR: 2977, 2934, 2870, 1723, 1479, 1450, 1392, 1366, 1254, 1142, 844, 751 cm$^{-1}$.

*General Procedure for the Preparation of HPC-PCL-PAA by Removal of tert-Butyl Groups Using Acidolysis with Trifluoroacetic Acid.* HPC-PCL-PtBA (**6**, 150 mg, ca. 1.2 mmol of t-BA units) was allowed to dissolve in $CH_2Cl_2$ (10 mL) for 15 min. Trifluoroacetic acid (TFA; 1.5 mL, 20 mmol) was added, and the reaction was stirred at ambient temperature for 12 h, after which the $CH_2Cl_2$ and TFA were removed via rotary evaporation. The polymer was redissolved in THF:water (1:1, 40 mL) and dialyzed against deionized water (MWCO 3500 Da) for 2 days. The polymer (64 mg) was obtained by lyophilization. Polymers **3**, **4**, **5**, and **7** were deprotected similarly, using 10−20 equiv of TFA/tBA unit. $^1$H NMR ($D_2O$): $\delta$ 1.5−2.0 (br, 2H, −C$H_2$CH(COOH)−), 2.2−2.6 (br, 1H, −CH$_2$C$H$(COOH)−), 10.69 ppm (s, H, −CH$_2$CH-(COO$H$)−). $^1$H NMR ($D_2O$:THF (1:1)): $\delta$ 0.89 (br), 1.14 (s, −CH(C$H_3$)OH or −CH(C$H_3$)OCH$_2$−), 1.28 (s, −CH(C$H_3$)-OCO−), 1.39 (s, −OCO(CH$_2$)$_2$C$H_2$(CH$_2$)$_2$− or remains of −C(C$H_3$)$_3$), 1.5−2.0 (br, −C$H_2$CH(COOH)−), 2.29 (t, −OCOC$H_2$-(CH$_2$)$_4$−)), 2.3−2.6 (br, CH$_2$C$H$(COOH)−), 4.05 ppm (t, −OCO(CH$_2$)$_4$C$H_2$OCO−). FT-IR: 3600−2400, 2931, 1700, 1451, 1412, 1235, 1161, 1106, 1056, 798 cm$^{-1}$.

*Suspension in Water: General Procedure.* In a typical suspension experiment, the amphihilic polymer (50.0 mg) was mixed in THF (40 mL) and deionized water (10 mL) to a polymer concentration of 1.0 mg mL$^{-1}$. When the polymer was dissolved, water (50 mL) was added dropwise to the solution during 2 h to promote the hydrophilic block to occupy the shell of the molecule and the hydrophobic to stay in the interior region. The solution was stirred overnight, and the THF was removed through dialysis against deionized water for 1 day. The volume after dialysis decreased to 70 mL (0.71 mg mL$^{-1}$), and the solution was diluted with water to a polymer concentration of 0.38 mg mL$^{-1}$. A solid sample was achieved from lyophilized water solution.

*Cross-Linking in Water of HPC-PCL-PAA.* To a water suspension of HPC-PCL-PAA (**9**) (25.0 mg of polymer, 0.35 mmol of acrylic acid units), 1-(3-(dimethylamino)propyl)-3-ethylcarbodiimide methiodide (103 mg, 0.35 mmol) in 5 mL of water was added dropwise. After 15 min, 2,2′-(ethylenedioxy)bis(ethylamine) (25.7 mg, 0.17 mmol) in 5 mL of water was added dropwise, and the cross-linking reaction was allowed to proceed overnight at ambient temperature. The solution was dialyzed with water for 2.5 days to remove byproducts from the cross-linking reaction. A solid-state sample was achieved by lyophilization of the cross-linked polymer. FT-IR: 3600−2400, 3280, 2930, 2870, 1711, 1635, 1547, 1447, 1392, 1350, 1245, 1168, 1088, 802 cm$^{-1}$.

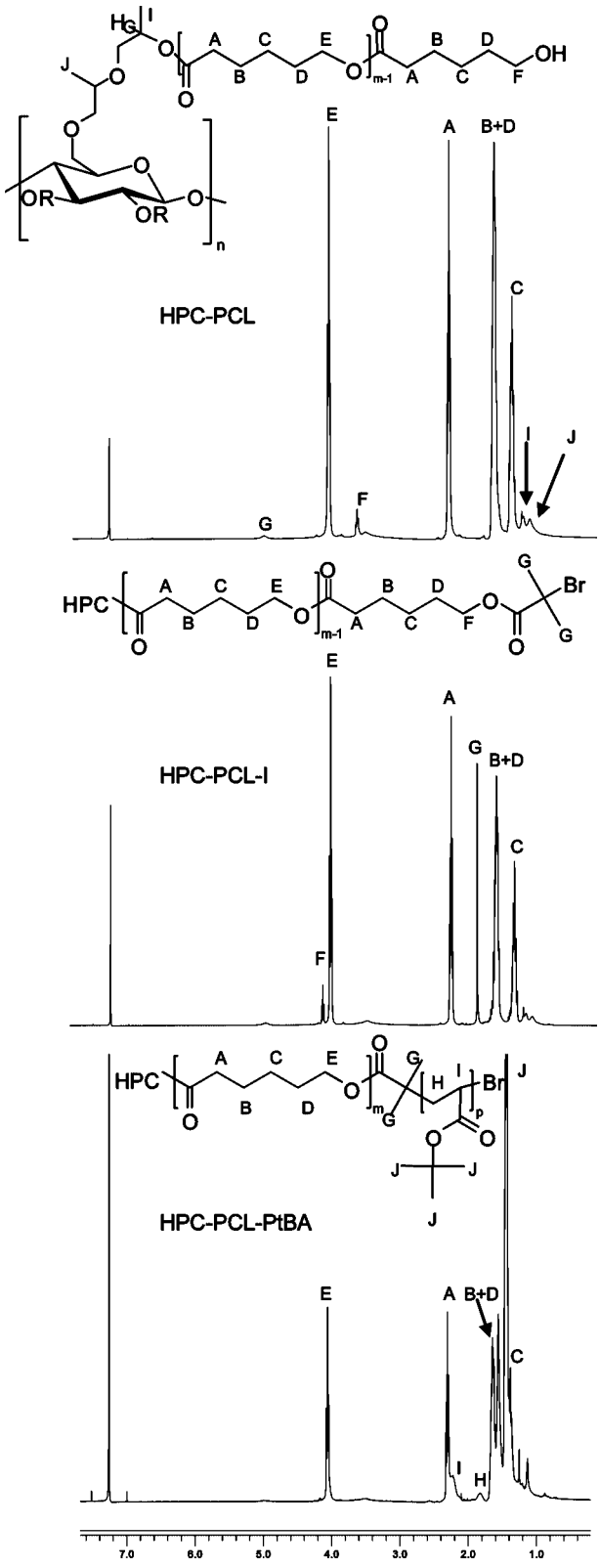


**Figure 2.** $^1$H NMR spectra of HPC-PCL (upper), HPC-PCL-I (middle), and HPC-PCL-PtBA (lower) (all in $CDCl_3$).

**Loading of Pyrene.** *A. Liquid−Liquid Transfer of Pyrene from Organic Phase to Water Phase.* Pyrene (5.0 mg) was dissolved in dichloromethane (2.0 mL) in a 7 mL glass vial, and a water solution of **9** (2.0 mL, 0.5 mg mL$^{-1}$) was added. The vial was tightly sealed and left without stirring for 2 weeks in the absence of light, after which the UV absorbance of the water phase was measured. A blank sample, containing an identical organic phase, but no amphiphilic polymer in the water phase, was also prepared and treated similarly.

*B. Loading of Pyrene through Cross-Linking of HPC-PCL-PAA.* Two different loadings of pyrene were attempted: 1.5 and 0.6 mg. Amphiphilic polymer **10** (7.5 mg; 105 $\mu$mol of acrylic acid units) was mixed in THF (11.25 mL) containing pyrene (1.5/0.6 mg) and deionized water (3.75 mL) to a polymer concentration of 0.5 mg mL$^{-1}$. The polymer was allowed to dissolve for 12 h, after which water (15 mL) was added dropwise to the solution during 12 h. 1-(3-(Dimethylamino)propyl)-3-ethylcarbodiimide methiodide (30.9 mg, 105 $\mu$mol) in 10 mL of THF/$H_2O$ (1/1 v/v) was added dropwise, and the solution was allowed to stir 12 h. 2,2′-(Ethylenedioxy)bis(ethylamine) (7.8 mg, 53 $\mu$mol) in 10 mL of THF/$H_2O$ (1/1 v/v) was added dropwise, and the cross-linking reaction was allowed to proceed for 48 h. The UV absorbance was measured (using deionized $H_2O$ as a reference), and the cross-linked amphiphile was dialyzed against deionized $H_2O$ for 48 h. During dialysis, the UV absorbance of the dialysis solution was measured at certain time intervals to monitor the pyrene content.

## Results and Discussion

Hydroxypropylcellulose (HPC) is a modified cellulose with a number of propylene oxide units on the anhydroglucose hydroxyl groups. This modification changes the properties of the cellulose, for example the solubility in organic solvents increases, but the number of hydroxyl end groups is unaffected. The HPC for this study has a calculated molar substitution (MS) of propylene oxide units of 2.9, which means that there are on average 2.9 propylene oxide units per anhydroglucose unit. Analysis using SEC with THF as the mobile phase gave $M_n$ = 25 150 g mol$^{-1}$ and a polydispersity index (PDI) of 2.5, which diverges from the molecular weight averages reported by the manufacturer ($M_n$ = 10 000 g mol$^{-1}$, $M_w$ = 80 000 g mol$^{-1}$). However, the values obtained using SEC are the polystyrene-equivalent molecular weights, and the calibration method does not provide absolute values due to the difference in hydrodynamic volume of linear polystyrene and HPC. HPC is used in biomedical applications, such as tablets where it acts as binder and release agent of the active compound, and its biocompatibility has been thoroughly studied.[42–44]

**Ring-Opening Polymerization of ε-Caprolactone from Hydroxypropylcellulose.** HPC was used as a macroinitiator for the ring-opening polymerization of ε-caprolactone (CL) in the synthesis of a high molecular weight comb polymer containing a cellulose backbone and poly(ε-caprolactone) (PCL) grafts (Scheme 1). The ROP was allowed to proceed at 110 °C for 2.5 h in 80 wt % toluene using $Sn(Oct)_2$ as catalyst. No drying of the CL was performed since the HPC would contribute with moisture although extensive drying of the sample had been conducted (24 h at 50 °C under vacuum). Instead, the comb polymer was separated from PCL homopolymer using dialysis in THF against THF. The ROP was allowed to proceed for 2.5 h until the stirrer bar was unable to move due to the high viscosity of the reaction mixture. At this point the monomer conversion was determined by $^1$H NMR spectroscopy and calculated to 84%. SEC of the resulting mixture of HPC-PCL and PCL homopolymer revealed a high molecular weight fraction and a smaller lower molecular weight fraction (Figure 1), which probably consisted of homopolymer, since no other impurities could be seen using $^1$H NMR. During the dialysis step, the weight fraction of homo-PCL decreased from 27 to 12 wt % (calculated from RI SEC trace); however, the final remains did not disappear. The number molecular weight-average of HPC-PCL is considerably higher than that of the unmodified HPC; cf. $M_n$ 158 700 and 25 200 g mol$^{-1}$, respectively. The instrument was calibrated using linear polystyrene standards, which suggests that the true values probably are significantly larger due to the comb architecture of HPC-PCL. The molecular weight distribu-

**Scheme 2. Functionalization with 2-Bromoisobutyryl Bromide on the HPC-PCL End Groups**

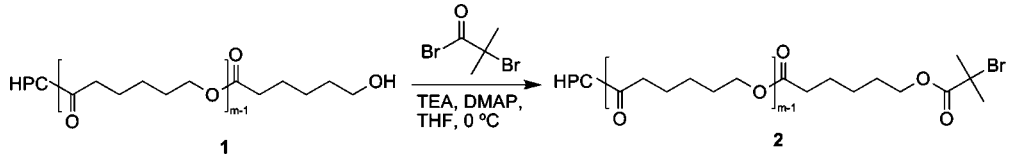


**Scheme 3. ATRP of *tert*-Butyl Acrylate from the HPC-PCL Macroinitiator**

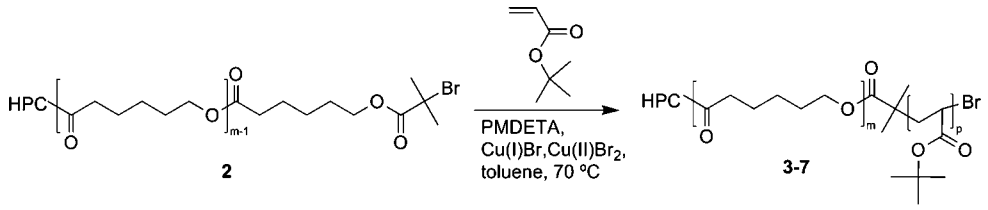


tion is somewhat narrowed when ROP is performed from HPC (Table 1).

The success of the grafting can be monitored by $^1$H NMR spectroscopy. In the HPC-PCL spectrum, peaks from both HPC and PCL are visible, and the grafting can be confirmed since the methyl group in a propoxy unit connected to a CL unit shifts upward, and a splitted peak is observed at 1.12 and 1.21 ppm (Figure 2, upper spectrum, peaks J and I).[31] The grafting density of PCL can be approximated by comparing the integral values of these peaks since the molar substitution of proxy groups is known (2.9 propoxy groups/anhydroglucose unit). The calculation gives 0.38, which is equal to 1.1 PCL grafts/anhydroglucose unit. However, this is most certainly an underestimation since the unmodified hydroxyl group on the anhydroglucose units on HPC, without a propoxy spacer, also can initiate polymerization of CL. At 5.00 ppm, a methine proton, also from a propoxy unit connected to a CL unit, can be seen (peak G) which further proves the grafting. The average degree of polymerization (DP) of the PCL grafts was calculated to 11 from the $^1$H NMR spectrum by comparing the integral value of the methylene end group at 3.64 ppm (peak F) and the value of the peak corresponding to the polymer analogue at 4.05 ppm (peak E). This indicates that almost all of the hydroxyl groups in HPC, more than 1.1/anhydroglucose unit, initiated polymerization of CL since a DP of 10 was aimed for. A melting transition could be observed in the DSC thermogram of HPC-PCL at 41 °C.

**Synthesis of Macroinitiator HPC-PCL-I.** In order to convert the PCL end groups into ATRP initiators, the hydroxyl groups of HPC-PCL were functionalized with 2-bromoisobutyryl bromide, which is an initiator suitable for acrylate monomers. To thoroughly dissolve HPC-PCL, the polymer was stirred in THF at 60 °C overnight. The functionalization was performed at 0 °C (water/ice bath), and the HPC-PCL solution was allowed to cool down slowly prior to addition of the reagents. The reaction was conveniently monitored using $^1$H NMR spectroscopy, since the resonance of the methylene group adjacent to the end hydroxyl group shift from 3.64 to 4.17 ppm during the functionalization step. The reaction was terminated after 2 h since no trace of the methylene resonance at 3.64 ppm could be observed.

The $^1$H NMR spectrum in Figure 2 (middle spectrum) only shows the initiator-functionalized end group (peak F), and it is therefore assumed that the reaction had reached almost completion. The methyl groups of the bromo ester group resonate at 1.92 ppm (peak G), and the integral values of the PCL arms are intact, indicating that no hydrolysis of the arms occurred. The SEC values of HPC-PCL-I are somewhat lower than those

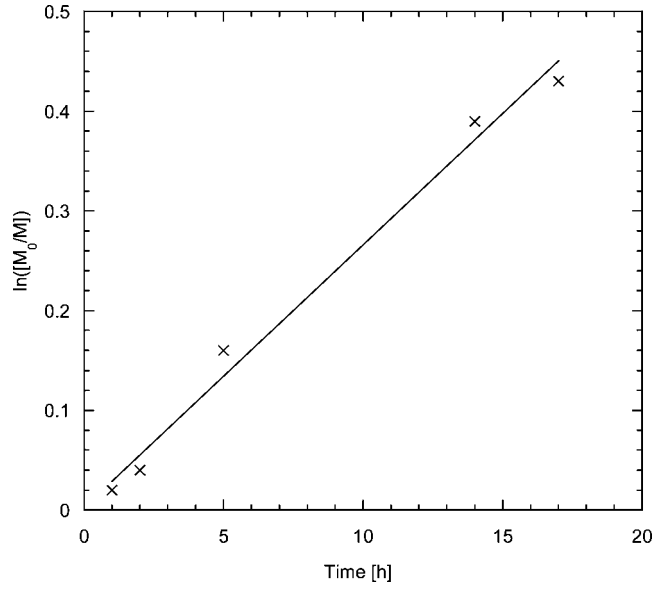


**Figure 3.** Semilogarithmic plot (ln([$M_0$/M])) vs time for the ATRP of t-BA initiated by HPC-PCL-I. Calculated from $^1$H NMR.

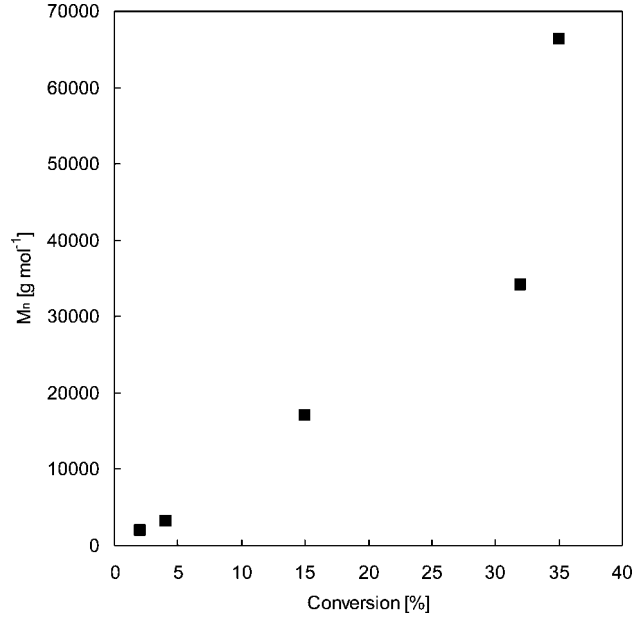


**Figure 4.** $M_n$ of the PtBA blocks vs conversion. Calculated from $^1$H NMR.

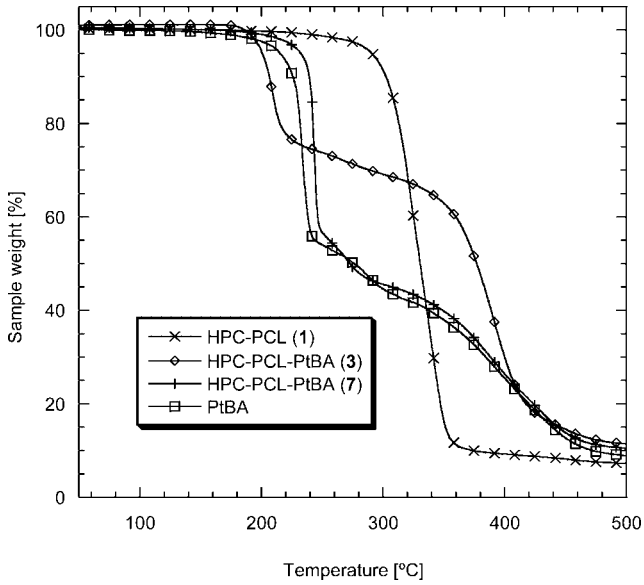


**Figure 5.** TGA thermogram showing the degradation under $N_2$ of HPC-PCL (**1**), HPC-PCL-PtBA (**3**), HPC-PCL-PtBA (**7**), and a homopolymer of PtBA.

of HPC-PCL, which might depend on a smaller hydrodynamic volume of HPC-PCL-I or the uncertainty of the SEC calibration system. The linear fraction of PCL could hardly be observed in the SEC trace after the conversion, which probably is due to the precipitation step, which is responsible for certain fractionation (Figure 1). In the FT-IR spectrum of HPC-PCL-I, a peak at 630 $cm^{-1}$ appears, which is not present in the FT-IR spectrum of HPC-PCL and can be attributed to the C−Br stretching mode. A melting transition could still be seen, although it was lowered from 41 to 33 °C when HPC-PCL was converted to HPC-PCL-I, which probably is due to the increased mobility of the PCL chains and less hydrogen bonding.

**ATRP from the Macroinitiator.** The macroinitiator HPC-PCL-I was used for copper-mediated ATRP of *tert*-butyl acrylate (t-BA). All polymerizations reactions were prepared with the same amounts of reactants, and the lengths of the PtBA blocks were varied through termination at different time intervals. In a typical experiment, the macroinitiator was added to the reaction mixture containing monomer, solvent, and ligand and was allowed to completely dissolve through heating it to 70 °C for ca. 10 min before the reaction was started through addition of copper salts and degassing (Scheme 3). $Cu(II)Br_2$ (20%) was added to the reaction mixtures, and they were diluted with 50 wt % toluene to decrease the concentration of propagating radicals and thus to slow down the polymerization. The t-BA conversion was measured using $^1H$ NMR spectroscopy after the predetermined polymerization time had elapsed. The monomer conversion was kept under 35% to minimize intermolecular coupling reactions between growing comb polymers due to the increased viscosity and lower mobility of the comb polymers at higher conversions. The ATRP of t-BA follows first-order kinetics with respect to monomer concentration; i.e., the number of propagating radicals is relatively constant, as can be seen in the plot in Figure 3.

The DPs of the PtBA blocks were calculated from $^1H$ NMR spectroscopy by comparing the unique resonance of the PCL protons at 4.06 ppm (lower spectrum, peak E) and the integral values of the *tert*-butyl moieties at 1.44 ppm (peak J), which are displayed in Table 2. As can be seen in Figure 4, the ATRP of PtBA is controlled up to 32% monomer conversions, after which the control is lost. However, the integral of such a high DP block makes the comparison with the low DP PCL block somewhat unreliable due to the large difference in the integral values. SEC was used to characterize the HPC-PCL-PtBA with the shortest PtBA block (sample **3**), and it was found that the number molecular weight average has increased ($M_n$) and a lowering of the PDI (Table 2). The molecular weight values obtained are polystyrene-equivalent molecular weights, and since the hydrodynamic volume of the comb polymer probably is lower than that of linear polystyrene having the same molecular weight, the values are most probably an underestimation. No detectable traces of linear PtBA could be found in the SEC trace of sample **3**, and it was assumed that presence of nongrafted PtBA was limited. SEC was only used for the HPC-PCL-PtBA having the shortest PtBA block due to the high molecular weights of the HPC-PCL-PtBA with higher DPs, which fall outside the rage of the calibration curve and could clog the columns due to the lower solubility.

Size characterization of the comb block copolymers was performed in solution with dynamic light scattering (DLS) in THF. The *Z*-average translational diffusion coefficient was used to calculate the diameters of the molecular coils, assuming a spherical geometry.[45] The results of the light scattering corroborate the SEC results of samples **1** and **2**, i.e., the hydrodynamic diameters, represented by the *Z*-average diameter, decreases when HPC-PCL is converted to HPC-PCL-I. The sizes of the molecular coils generally increased with increasing graft length of the PtBA block, samples **3**−**7**, as can be seen in Table 2. However, the shortest blocks show larger sizes and PDIs, which could depend on some termination reactions before the persistent radical effect is established or influence of the shape of the molecular coil.

The PtBA content in the block copolymers was easily estimated using thermal gravimetric analysis (TGA) thanks to the complete weight loss of isobutene at ca. 250 °C.[46] The remaining polymer is unaffected at this temperature since the degradation onset temperature of HPC-PCL is ca. 300 °C. The difference in PtBA content between the block copolymers is reflected in the thermograms (Figure 5), showing HPC-PCL (**1**), HPC-PCL-PtBA (**3**), HPC-PCL-PtBA (**7**) (shortest and longest polymerization time), and a homopolymer of PtBA.

A homopolymer of PtBA was analyzed using TGA to verify that the experimental values of the isobutene weight loss could be used to calculate the residual PAA block weight. As can be seen in Table 3, the calculated and experimental weight loss of isobutene are in good agreement, and the experimental weight loss values were therefore used to calculate the weight fraction of PtBA in the block copolymers. The high PtBA contents of samples **5**−**7** may appear odd, but the DPs of the PtBA blocks in these polymers are 10−50 times higher than that of the PCL block, which in turn represents a very small weight fraction of the sample. This method does not give enough accuracy to determine the weight of such a small HPC-PCL fraction.

The HPC-PCL-PtBA samples were analyzed using DSC. In the DSC thermograms of the comb block copolymers with the shortest PtBA blocks (**3** and **4**), no transitions could be observed, which could depend on a non-phase-separated morphology. This might be due to that the PCL and PtBA blocks are too short and the mobility is high, affecting both blocks. However, in sample **5** a very sharp melting transition was observed at 41 °C, but it was not possible to distinguish a PtBA glass transition. In samples **6** and **7** no melting transitions could be detected for the PCL blocks, which could be due to that the heating/cooling rate is too high to promote crystallization of the PCL block in these samples. In the second heating cycles of these samples, the glass transition of PtBA is dominating the DSC thermograms. This suggests a phase-separated morphology in samples **5**−**7**.

**Table 3. Composition of the Block Copolymers and a Homopolymer of PtBA Analyzed with TGA and Thermal Properties Obtained from DSC**

| sample no. | sample | DP PtBA | calcd wt loss[a] (%) | exptl wt loss[b] (%) | wt % PtBA | thermal transitions |
|---|---|---|---|---|---|---|
| | PtBA | 66 | 44 | 43 | 100 | |
| **3** | HPC-PCL-PtBA | 15 | 24 | 22 | 51 | not observed |
| **4** | HPC-PCL-PtBA | 25 | 29 | 28 | 66 | not observed |
| **5** | HPC-PCL-PtBA | 133 | 40 | 42 | 98 | $T_{m,PCL} = 41$ °C |
| **6** | HPC-PCL-PtBA | 266 | 42 | 44 | ~100 | $T_{g,PtBA} = 37$ °C |
| **7** | HPC-PCL-PtBA | 518 | 43 | 44 | ~100 | $T_{g,PtBA} = 33$ °C |

[a] The calculated weight loss values were achieved from DP values, obtained by $^1$H NMR, and the maximum possible HPC content obtained by gravimetry. [b] The weight loss values were determined at the inflection points after the first weight loss (close to 250 °C).

**Scheme 4. Deprotection of the *tert*-Butyl Group Using Trifluoroacetic Acid To Form a Poly(acrylic acid) Block**

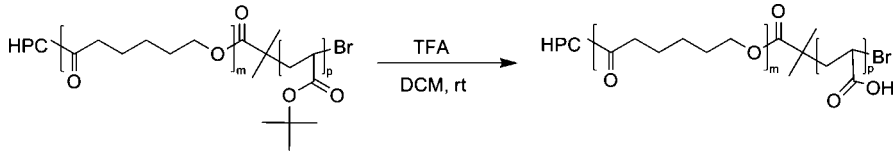


**Table 4. HPC-PCL-PtBA Samples That Were Successfully Deprotected to HPC-PCL-PAA Using Trifluoroacetic Acid and Subsequently Suspended in Water**

| | | | | | | DLS[c] | |
|---|---|---|---|---|---|---|---|
| sample no. | sample | NMR[a] DP PtBA | DLS[b] *Z*-average (nm) | sample no. | sample | Z-average (nm) | PDI[d] |
| **5** | HPC-PCL-PtBA | 133 | 69.6 | **8** | HPC-PCL-PAA | 62.8 | 0.29 |
| **6** | HPC-PCL-PtBA | 266 | 86.3 | **9** | HPC-PCL-PAA | 129.5 | 0.31 |
| **7** | HPC-PCL-PtBA | 518 | 90.2 | **10** | HPC-PCL-PAA | 152.0 | 0.25 |

[a] Obtained using $^1$H NMR in $CDCl_3$. [b] Obtained in THF. [c] Obtained in water. [d] PDI for cumulative light scattering (0−1). Broad distributions show a PDI close to 1 and the more narrow the lower the PDI.

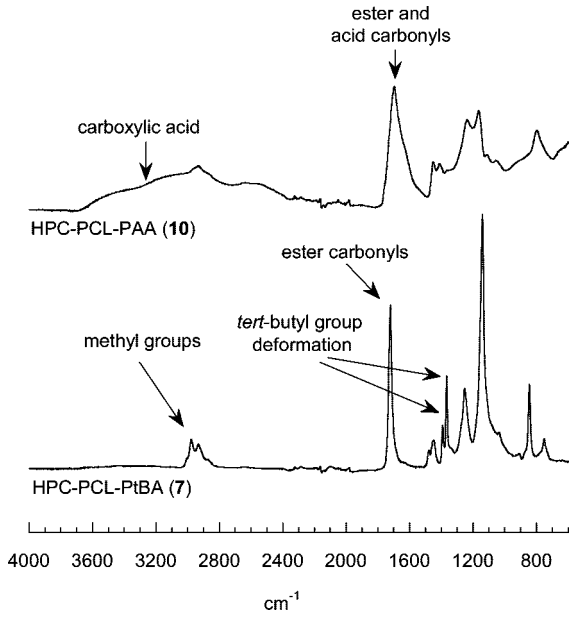


**Figure 6.** FT-IR spectra of HPC-PCL-PtBA (**7**) (lower) and HPC-PCL-PAA (**10**) (upper).

**Deptrotection of the PtBA Block.** The HPC-PCL-PtBA samples were subjected to mild acidolysis using excess of trifluoroacetic acid (TFA) according to an established method (Scheme 4).[46] This method is known to produce poly(acrylic acid) (PAA) after selectively cleaving off the isobutene moieties from poly(*tert*-butyl acrylate). It has earlier been shown that the PCL block is unaffected by the acidic treatment and that no degradation of the polyester occurs when using short reaction times at ambient temperature.[13]

During the course of the reaction, the solubility of the produced amphiphilic polymer changed, and precipitation was observed for the block copolymers with long PtBA blocks (samples **5**−**7**, see Table 4). The reaction was monitored using

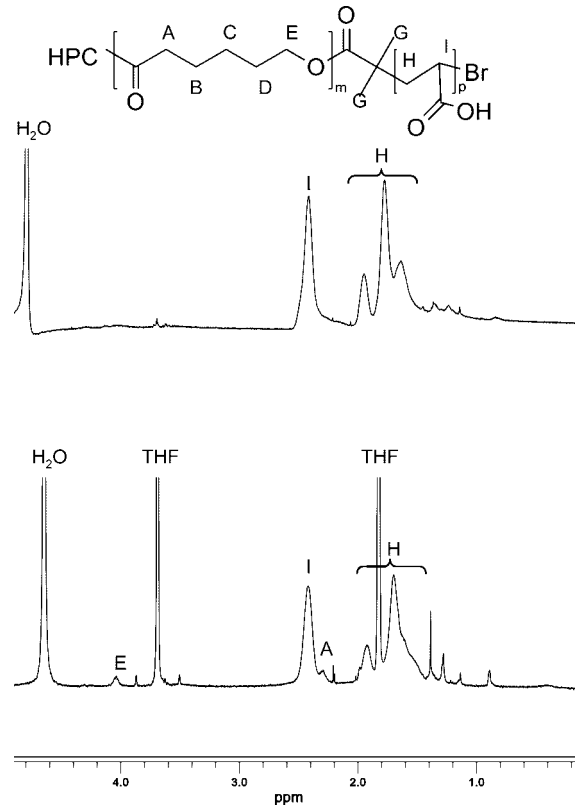


**Figure 7.** $^1$H NMR spectra of HPC-PCL-PAA (**10**) in $D_2O$ (upper spectrum) and $D_2O$:THF-$d_8$ 50:50 (lower spectrum).

FT-IR and $^1$H NMR spectroscopies. FT-IR was convenient, since the absorbance of the PAA block show distinct differences to those of the PtBA block. The PtBA block exhibits two sharp peaks at 1366 and 1392 $cm^{-1}$, which are originating from the deformation mode vibration of the *tert*-butyl group (Figure 6). After deprotection with TFA these peaks disappear completely.

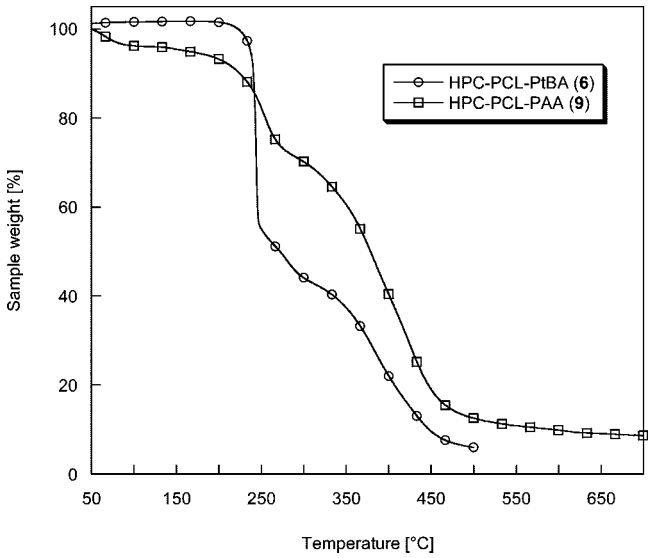


**Figure 8.** TGA thermograms of HPC-PCL-PtBA (**6**) and HPC-PCL-PAA (**9**).

Moreover, the carbonyl absorbance of HPC-PCL-PAA is shifted to lower wavenumbers (ca. 1700 $cm^{-1}$) compared to that of HPC-PCL-PtBA at 1720 $cm^{-1}$ due to the formation of acid carbonyl. However, the peak also becomes broader because of the carbonyl ester absorbance remaining in the PCL block. Another characteristic feature is the appearance of a broad peak, ranging from 2400 to 3600 $cm^{-1}$, originating from the carboxylic acid groups in the formed PAA block. The comb block copolymers with the shortest blocks (**3** and **4**) were more difficult to deprotect completely. Remains of the peaks at 1366 and 1392 $cm^{-1}$ could be seen although larger excess of TFA was used and prolonged reaction times were applied. The difficulty may depend on shielding of the shorter PtBA blocks inside the PCL blocks, making them inaccessible for deprotection. Attempts to deprotect the *tert*-butyl moieties using thermal treatment (employing the TGA setup) resulted in insoluble polymers.

It is a challenge to achieve representative $^1H$ NMR spectra of the HPC-PCL-PAA samples due to their amphihilic nature and relative high molecular weight, which make them sparingly soluble in common solvents for NMR spectroscopy. For example, when pure $D_2O$ was used for $^1H$ NMR spectroscopy of HPC-PCL-PAA, the concentration of sample required to achieve good resolution resulted in a physical gel in the NMR tube due to the hydrogen bonding between $D_2O$ and the polymer. The spectrum was recorded with 128 scans and is displayed in Figure 7 (upper spectrum). The PAA block is clearly visible, and it is obvious that the deprotection reaction was successful due to the absence of the peak from methyl resonances of the *tert*-butyl group at 1.44 ppm. The broad peaks from the PAA backbone are visible at 1.5−2.4 ppm (peaks H and I). However, no significant trace of the PCL block can be observed when $D_2O$ is used for the $^1H$ NMR spectroscopy.

THF-$d_8$ was added to the sample (50 vol %), and the mobility of the sample increased, since the gel-like behavior ceased. The spectrum recorded with this solvent mixture is shown in Figure 7 (lower spectrum). The peaks from the PAA block are still present, but with this solvent mixture some peaks from the PCL block can also be seen at 4.05 ppm (peak E) and 2.29 ppm (peak A).

TGA was another method to confirm the success of the deprotection reaction. The thermogram of HPC-PCL-PAA is different from that of its precursor HPC-PCL-PtBA; no sharp weight loss caused by the release of isobutene at 250 °C is shown (Figure 8). Instead, the thermogram of HPC-PCL-PAA is characterized by a less pronounced weight loss just above 250 °C, which is similar to the second weight loss of HPC-PCL-PtBA after an initial release of bound water at 100 °C. The remaining weight loss profile of HPC-PCL-PAA is identical to that of its precursor, which suggests that only the PtBA block was affected during the treatment with TFA.

The DSC traces of polymers **8**−**10** showed loss of water during the first heating cycles because of the amphiphilic polymers hygroscopic nature. The DSC trace of polymer **8** did not show any thermal transitions; however, the traces of polymers **9** and **10** showed clear glass transitions at 127 and 125 °C, respectively, which were attributed to the poly(acrylic acid) blocks.[47] In addition, polymer **9** showed a melting transition in the first heating cycle (62 °C), but this melting could not be observed in any other cycle. No sign of the PtBA glass transition could be observed in any of the samples.

The amphiphilic polymers were dissolved in a mixture of THF:water (4:1, v:v), and water was added dropwise to circumvent precipitation of the polymer. However, the samples with the shortest PAA blocks, samples **3** and **4**, were impossible to suspend in water, since the hydrophobic parts were too dominating, due to remains of *tert*-butyl groups. When a concentration of 0.5 mg $mL^{-1}$ was obtained, the mixture was dialyzed against deionized water for 2 days to remove the THF.

Analysis using DLS was performed on samples **8**−**10** in water, and it was found that in addition to centrifugation and filtering of the samples, neutralization with a small amount of $NaHCO_3$ was needed to prevent aggregation.[13] The two samples having longer PAA blocks (**9** and **10**) exhibited larger molecular sizes than their precursors, whereas the shortest (**8**) showed comparable sizes before and after deprotection. The small decrease of the size could depend on collapse of the HPC-PCL part during suspension in water due to low solubility. It should be noted that two different solvents were used during the DLS analysis, THF and water, which could affect the obtained sizes, in addition to the differences expected from the difference in the size of the molecular coil due to the relative "goodness" of the solvent, before and after deprotection.

**Cross-Linking.** The cross-linking of the amphiphilic polymers was performed through addition of 1-(3-(dimethylamino-)propyl)-3-ethylcarbodiimide methiodide and subsequently the cross-linker 2,2′-(ethylenedioxy)bis(ethylamine) (**1**, **2** in Scheme 5). Different concentrations of the amphiphilic polymers in water were applied to achieve different sizes of the cross-linked micelles. The extent of cross-linking was varied to 25, 50, and 100% relative to the acrylic acid units. The data for the cross-linking experiments are showed in Table 5.

As can be seen in Table 5, the concentration of the amphiphilic polymer and the cross-linking density have an impact on the resulting size of the cross-linked nanoparticles. Swelling of the formed hydrogel is probable and could be responsible for the larger sizes obtained for the cross-linked molecules in water.[47] It is likely that intermolecular cross-linking occurs to some extent, since most of the cross-linked amphiphilic polymers are larger than their precursors and show wider size distributions. The only sample in which precipitation of the cross-linked amphiphilic polymer could be observed was sample **8a**, which reached a size of 320 nm. When a low cross-linking density is used in combination with dilute samples, the smallest size is obtained 89 nm (sample **10d**). This might be due to that very little intermolecular cross-linking occurs using these reaction conditions.

The cross-linking reaction could be observed by using FT-IR on lyophilized samples. The success of the cross-linking reaction is easily seen by the appearance of amide bands (I and II) at 1636 and 1550 $cm^{-1}$ (Figure 9).[48] However, no significant

**Scheme 5. Unimolecular Cross-Linking of HPC-PCL-PAA with a Diamine for the Formation of a Poly(acrylamide) Hydrogel Shell**

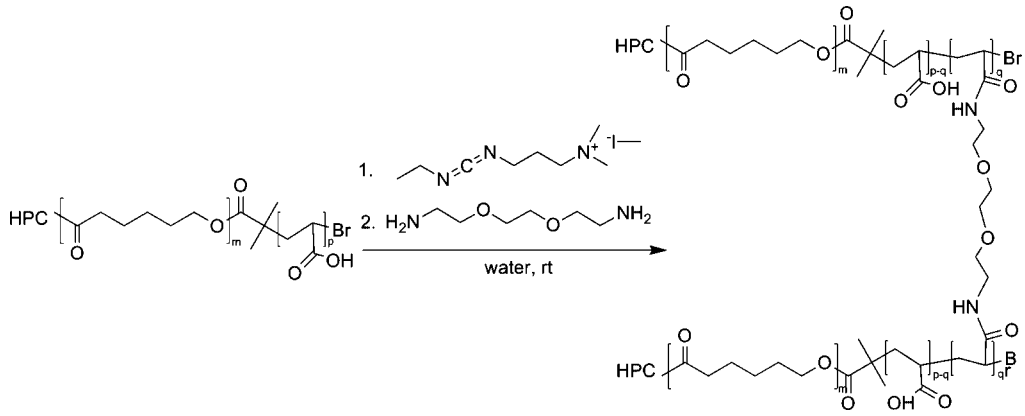


**Table 5. Conditions for the Cross-Linking Experiments and Size Data Obtained by Using DLS in Water**

| | | | DLS[b] | | | DLS[b] | |
|---|---|---|---|---|---|---|---|
| cross-linked amphiphile | extent of cross-linking (%) | NMR[a] DP PAA | *Z*-average precursor (nm) | PDI | concn cross-linking (mg mL$^{-1}$) | *Z*-average cross-linked amphiphile (nm) | PDI |
| **8a** | 100 | 133 | 62.8 | 0.29 | 0.31 | 320.0 | 0.54 |
| **9a** | 100 | 266 | 129.5 | 0.31 | 0.37 | 196.8 | 0.29 |
| **9b** | 100 | 266 | 129.5 | 0.31 | 0.26 | 235.3 | 0.32 |
| **10a** | 100 | 518 | 152.0 | 0.25 | 0.38 | 197.5 | 0.27 |
| **10b** | 100 | 518 | 152.0 | 0.25 | 0.23 | 132.3 | 0.25 |
| **10c** | 50 | 518 | 152.0 | 0.25 | 0.23 | 208.3 | 0.44 |
| **10d** | 25 | 518 | 152.0 | 0.25 | 0.21 | 89.3 | 0.40 |

[a] DP for the HPC-PCL-PtBA precursor, obtained from $^1$H NMR in $CDCl_3$. [b] Obtained in water. PDI for cumulative light scattering (0−1). Broad distributions show a PDI close to 1, and the more narrow the lower the PDI.

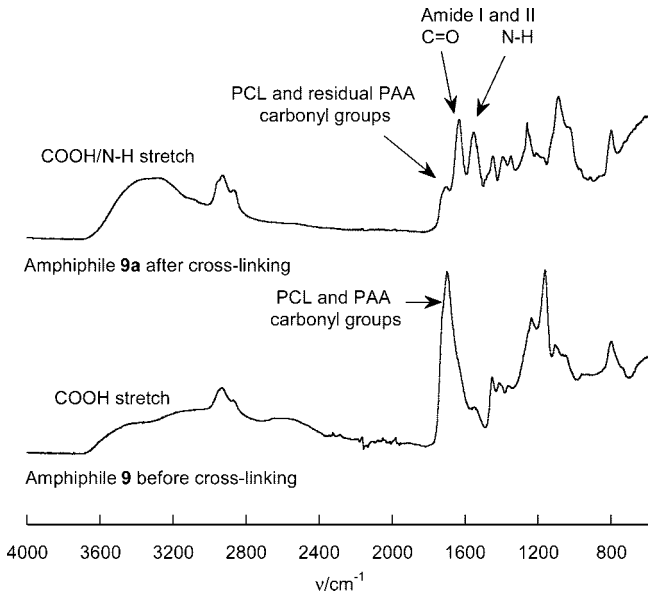


**Figure 9.** FT-IR of amphiphile (**9**) before (lower) and after cross-linking with diamine (**9a**) (upper).

differences in the amide absorption could be observed when different extents of cross-linking were attempted. This could be due to limited diffusion of the cross-linking agent, 2,2′-(ethylenedioxy)bis(ethylamine), into the interior regions of the shell, during the course of the cross-linking reaction. A buildup of high cross-linking density of the outer shell region and less dense cross-linking in the interior regions of the shell could be the consequence. This could also explain the residual PAA absorbance that is seen in the absorbance of 100% cross-linked amphiphile (**9**) (Figure 9).

**AFM Characterization.** AFM characterization of the block copolymers and cross-linked amphiphilic polymers in the dry state was performed on mica surfaces using tapping-mode atomic force microscopy (TM-AFM). The block copolymers were spin-coated from THF solutions, and the cross-linked amphiphilic polymers were drop-cast from water and subsequently dried onto mica surfaces. The block copolymers were not easily visualized as single molecules, but when a concentration of 0.1 mg mL$^{-1}$ was used for the casting, it was possible to observe small aggregates of the molecules. The TM-AFM height image is showed in Figure 10. As can be seen in Figure 10, the height scale is only 5.0 nm, which suggests a thin coverage of a few molecules or possibly single molecules. The size of the features is ca. 70−100 nm, which is similar to that obtained by DLS (90 nm). However, earlier studies show that the molecules usually collapse in the dry state, when spin-cast onto a surface and dried, which could explain the smaller sizes.[30]

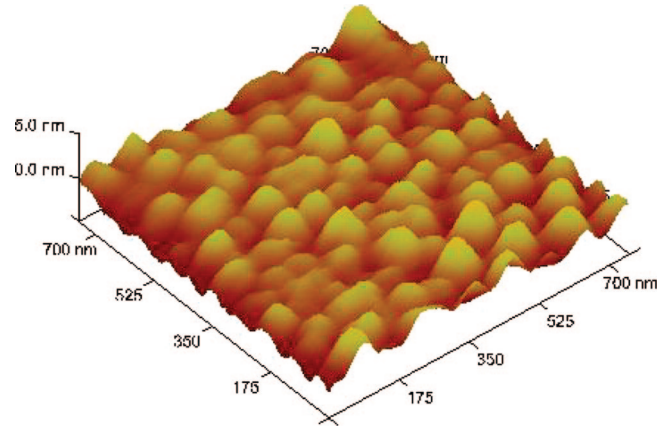


**Figure 10.** TM-AFM height image of HPC-PCL-PtBA (**7**) spin-cast from THF (0.1 mg mL$^{-1}$) onto mica.

Cross-linked amphiphilic polymers were also subjected to AFM analysis. However, the smaller nanoparticles were not readily visualized using AFM. One of the cross-linked samples that probably consists of both unimolecular and aggregating polymer, **10a**, formed some interesting features when dried on mica (Figure 11).

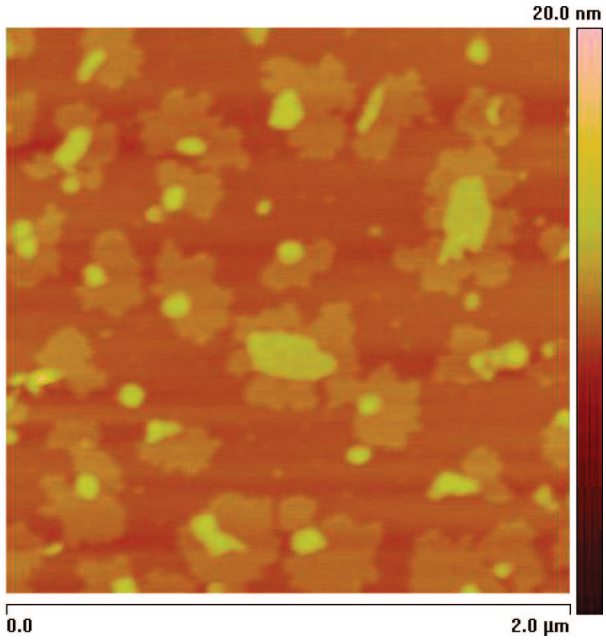


**Figure 11.** TM-AFM height image of cross-linked amphiphilic polymer (**10a**) dried on mica.

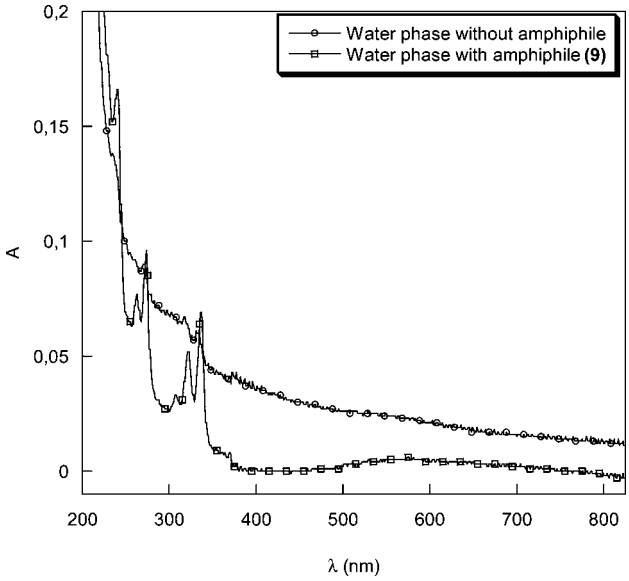


**Figure 12.** UV absorbance of water phases after 2 weeks of pyrene transfer: the line with circled markers represents water phase without amphiphilic polymer, and the line with squared markers represents amphiphile-containing water phase.

It is possible that the lower height corona, surrounding the higher features in the image, is the cross-linked shell, which collapse upon drying. This polymer should probably spread out on the surface due to similar polarity of the shell and mica. The higher parts (a few nanometers high) are probably the HPC-PCL part, which gather in the center parts of the micelle to avoid contact with the bad solvent. It is possible that the smallest features are single unimolecular micelles; however, the features are probably aggregates formed during cross-linking or during drying on the substrate, which show differently sized phases. The sizes of the features are polydisperse, which makes it hard to estimate their size and speaks for aggregation during drying in addition to certain aggregation during cross-linking. However, the smaller features could be single amphiphilic block copolymers since the size is approximately equal to that of the swollen nanoparticle in solution (ca. 200 nm).

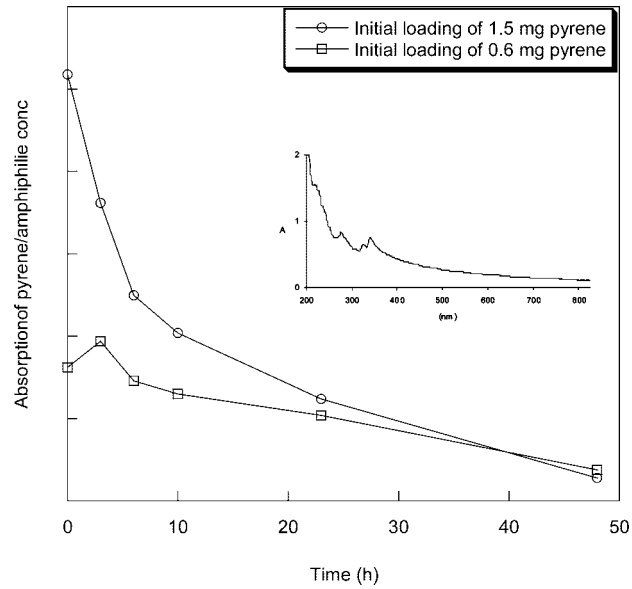


**Figure 13.** UV absorbance at 337 nm (pyrene) during dialysis against water for cross-linked amphiphiles with different initial pyrene loading. The inset shows the absorbance after 23 h for the amphiphile with the higher loading of pyrene.

**Loading of Pyrene in the Amphiphiles.** It is of interest to investigate whether the amphiphilic comb copolymers can solubilize a hydrophobic compound, since most drugs are hydrophobic, which need amphiphilic carriers to deliver them in an aqueous environment. Pyrene is an unreactive, hydrophobic, water-insoluble compound ($6.57 \times 10^{-7}$ mol $L^{-1}$),[49] which is rewarding to use for loading experiments, thanks to its UV activity. Loading of pyrene was conducted using two different strategies: liquid−liquid transfer of pyrene from organic phase to amphiphile phase (A) and incorporation of pyrene during suspension of non-cross-linked amphiphile in water with subsequent cross-linking (B). Route A was conducted through dissolving pyrene in dichloromethane in a vial and adding the water-suspended amphiphile on top (equal volumes). The two phases were allowed to stand at ambient temperature, without stirring, for 2 weeks, after which the UV absorbance of the water phase was measured. A blank sample, without amphiphilic polymer in the water phase, was treated similarly, and their absorption spectra are shown in Figure 12. As can be seen in Figure 12, the absorbance of the amphiphile-containing water phase is more detailed than the one without amphiphilic polymer, suggesting that the amphiphlies have a solublizing effect on the pyrene molecules. The concentration of pyrene is hard to determine due to the fact that the extinction coefficient of pyrene in water ($\varepsilon$, Lambert−Beer's law) is unknown and cannot be measured easily. The absorption spectrum of the amphiphile-containing water phase is, however, very similar to that of pyrene in THF.

When using route B, the cross-linking reaction was performed in the mixture of THF:water, which was obtained after addition of water to the dissolved amphiphile. No removal of THF prior to cross-linking of the micelles was performed, since this was believed to release the pyrene molecules in the micelles simultaneously. Instead, the cross-linking was performed in the existing mixture, and the THF was removed through dialysis against deionized water, during which the UV absorbance was measured at certain times intervals. The concentration of amphiphilic polymer was kept low (0.15 mg $mL^{-1}$), since it was observed that higher concentrations generated precipitation during the cross-linking reaction. During the dialysis, the concentration of amphiphilic polymer will change due to the

replacement of THF and cross-linking reagents, and the volume inside the dialysis bag was therefore measured and corrected for in the UV measurements (Figure 13).

Pyrene exhibits a local UV absorption maximum at ~337 nm, and this peak was used to monitor the diffusion of pyrene from the amphiphilic polymers into the water phase. As can be seen in Figure 13, the initial loading of 1.5 mg sample shows a higher UV absorption than that of the lower loading. However, this high loading decreases more rapidly than the lower, and these two loadings converge to a similar value after ~24 h. This is the time normally used to remove the byproducts of the cross-linking reaction. After 48 h, there is still pyrene left in the micelles, since the UV absorption spectra show the characteristic pyrene peaks. However, certain precipitation of the cross-linked micelles could be observed at this time.

## Conclusions

High molecular weight comb block copolymers, consisting of a hydroxypropylcellulose backbone, inner blocks of PCL and outer blocks of different lengths of PtBA were successfully synthesized using a combination of ROP and ATRP. The PtBA length could be controlled up to 32% monomer conversion by applying different polymerization times and the diameters of the molecular coil in solution, measured as the *Z*-average, increased with increasing polymerization time (~60−90 nm). The comb block copolymers consisting of more than 66 wt % PtBA were successfully deprotected using TFA to yield water-suspendable amphiphilic comb block copolymers, unimolecular micelles, with an outer PAA block. Cross-linking of the micelles using amidation could be detected with FT-IR and resulted in certain intermolecular cross-linking when the attempted cross-linking percentage was higher than 25%, and the amphiphile concentration was higher than 0.21 mg/mL. The sizes of the cross-linked micelles were in the range 89−320 nm obtained by DLS, and analysis using AFM implied that they had a phase-separated morphology. Initial loading experiments using pyrene in the amphiphilic polymers suggest that it is possible to solubilize small amounts of pyrene in water with these unimolecular micelles. We are currently investigating the encapsulation capacity of hydrophobic compounds of these comb block copolymers further and are focusing on tailoring the unimolecular micelles for drug delivery. The pH dependence of the comb block copolymers will also be studied.

**Acknowledgment.** We thank the Swedish Research Council, under grant 2006-3621, Wilhelm Beckers Jubileumsfond, and The Research Council of Norway within the NanoMat program, project "Dendritic nanoporousmaterials with multifunctionality (no. 163529/S10), for financial support. Niklas Nordgren and Erik Johansson, KTH, are thanked for assistance and discussions regarding AFM analysis. Lars-Erik Enarsson, KTH, is thanked for help with light scattering experiments. Josefina Lindqvist and Jarmo Ropponen are acknowledged for valuable scientific discussions.

## References and Notes

(1) Thurmond, K. B.; Kowalewski, T.; Wooley, K. L. *J. Am. Chem. Soc.* **1996**, *118* (30), 7239–7240.
(2) Nagasaki, Y.; Okada, T.; Scholz, C.; Iijima, M.; Kato, M.; Kataoka, K. *Macromolecules* **1998**, *31* (5), 1473–1479.
(3) Huang, H.; Remsen, E. E.; Kowalewski, T.; Wooley, K. L. *J. Am. Chem. Soc.* **1999**, *121* (15), 3805–3806.
(4) Zhang, Q.; Remsen, E. E.; Wooley, K. L. *J. Am. Chem. Soc.* **2000**, *122* (15), 3642–3651.
(5) Newkome, G. R.; Moorefield, C. N.; Baker, G. R.; Johnson, A. L.; Behera, R. K. *Angew. Chem., Int. Ed.* **1991**, *30* (9), 1176–1178.
(6) Hawker, C. J.; Wooley, K. L.; Fréchet, J. M. J. *J. Chem. Soc., Perkin Trans. 1* **1993**, *12*, 1287–1297.
(7) Stevelmans, S.; van Hest, J. C. M.; Jansen, J. F.; G, A.; van Boxtel, D. A. F. J.; de Brabander-van den Berg, E. M. M.; Meijer, E. W. *J. Am. Chem. Soc.* **1996**, *118* (31), 7398–7399.
(8) Heise, A.; Hedrick, J. L.; Frank, C. W.; Miller, R. D. *J. Am. Chem. Soc.* **1999**, *121* (37), 8647–8648.
(9) Cheng, G.; Boker, A.; Zhang, M.; Krausch, G.; Muller, A. H. E. *Macromolecules* **2001**, *34* (20), 6883–6888.
(10) Meier, M. A. R.; Gohy, J. F.; Fustin, C. A.; Schubert, U. S. *J. Am. Chem. Soc.* **2004**, *126* (37), 11517–11521.
(11) Meier, M. A. R.; Schubert, U. S. *J. Comb. Chem* **2005**, *7* (3), 356–359.
(12) Kreutzer, G.; Ternat, C.; Nguyen, T. Q.; Plummer, C. J. G.; Mnson, J.-A. E.; Castelletto, V.; Hamley, I. W.; Sun, F.; Sheiko, S. S.; Herrmann, A.; Ouali, L.; Sommer, H.; Fieber, W.; Velazco, M. I.; Klok, H.-A. *Macromolecules* **2006**, *39* (13), 4507–4516.
(13) Ternat, C.; Kreutzer, G.; Plummer, C. J. G.; Nguyen, T. Q.; Herrmann, A.; Ouali, L.; Sommer, H.; Fieber, W.; Velazco, M. I.; Klok, H.-A.; Manson, J.-A. E. *Macromol. Chem. Phys.* **2007**, *208* (2), 131–145.
(14) Rösler, A.; Vandermeulen, G. W. M.; Klok, H.-A. *Adv. Drug Delivery Rev.* **2001**, *53*, 95–108.
(15) Leobandung, W.; Ichikawa, H.; Fukumori, Y.; Peppas, N. A. *J. Appl. Polym. Sci.* **2003**, *87* (10), 1678–1684.
(16) Wang, J.-S.; Matyjaszewski, K. *J. Am. Chem. Soc.* **1995**, *117* (20), 5614–15.
(17) Kato, M.; Kamigaito, M.; Sawamoto, M.; Higashimura, T. *Macromolecules* **1995**, *28* (5), 1721–3.
(18) Wang, J.-S.; Matyjaszewski, K. *Macromolecules* **1995**, *28* (22), 7572–3.
(19) Carlmark, A.; Malmström, E. *J. Am. Chem. Soc.* **2002**, *124* (6), 900–901.
(20) Carlmark, A.; Malmström, E. E. *Biomacromolecules* **2003**, *4* (6), 1740–1745.
(21) Lee, S. B.; Koepsel, R. R.; Morley, S. W.; Matyjaszewski, K.; Sun, Y.; Russell, A. J. *Biomacromolecules* **2004**, *5* (3), 877–882.
(22) Lindqvist, J.; Malmström, E. *J. Appl. Polym. Sci.* **2006**, *100*, 4155–4162.
(23) Nyström, D.; Lindqvist, J.; Östmark, E.; Hult, A.; Malmström, E. *Chem. Commun.* **2006**, 3594–3596.
(24) Westlund, R.; Carlmark, A.; Hult, A.; Malmström, E.; Saez, I. M. *Soft Matter* **2007**, *3* (7), 866–871.
(25) Shen, D.; Huang, Y. *Polymer* **2004**, *45* (21), 7091–7097.
(26) Shen, D.; Yu, H.; Huang, Y. *J. Polym. Sci., Part A: Polym. Chem.* **2005**, *43* (18), 1099–4108.
(27) Vlcek, P.; Janata, M.; Latalova, P.; Kriz, J.; Cadova, E.; Toman, L. *Polymer* **2006**, *47* (8), 2587–2595.
(28) Shen, D.; Yu, H.; Huang, Y. *Cellulose* **2006**, *13* (3), 235–244.
(29) Kang, H.; Liu, W.; He, B.; Shen, D.; Ma, L.; Huang, Y. *Polymer* **2006**, *47* (23), 7927–7934.
(30) Östmark, E.; Harrisson, S.; Wooley, K. L.; Malmström, E. E. *Biomacromolecules* **2007**, *8* (4), 1138–1148.
(31) Shi, R.; Burt, H. M. *J. Appl. Polym. Sci.* **2003**, *89* (3), 718–727.
(32) Hafrén, J.; Córdova, A. *Macromol. Rapid Commun.* **2005**, *26* (2), 82–86.
(33) Lönnberg, H.; Zhou, Q.; Brumer, H.; Teeri, T.; Malmström, E.; Hult, A. *Biomacromolecules* **2006**, *7* (7), 2178–2185.
(34) Wang, C.; Tan, H.; Dong, Y.; Shao, Z. *React. Funct. Polym.* **2006**, *66* (10), 1165–1173.
(35) Yuan, W.; Yuan, J.; Zhang, F.; Xie, X. *Biomacromolecules* **2007**, *8* (4), 1101–1108.
(36) Hafrén, J.; Cordova, A. *Nord. Pulp. Pap. Res. J.* **2007**, *22* (2), 184–187.
(37) Daly, W. H.; Evenson, T. S.; Iacono, S. T.; Jones, R. W. *Macromol. Symp.* **2001**, *174*, 155–163.
(38) Stenzel, M. H.; Davis, T. P.; Fane, A. G. *J. Mater. Chem.* **2003**, *13* (9), 2090–2097.
(39) Hernandez-Guerrero, M.; Davis, T. P.; Barner-Kowollik, C.; Stenzel, M. H. *Eur. Polym. J.* **2005**, *41* (10), 2264–2277.
(40) Roy, D.; Guthrie, J. T.; Perrier, S. *Macromolecules* **2005**, *38* (25), 10363–10372.
(41) Barsbay, M.; Gueven, O.; Stenzel, M. H.; Davis, T. P.; Barner-Kowollik, C.; Barner, L. *Macromolecules* **2007**, 000
(42) Anon, *Fed. Regist.* **1964**, *29*, 12586.
(43) Block, L. H.; Lamy, P. P. *Pharm. Acta Helv.* **1969**, *44* (1), 44–53.
(44) Nakamoto, A.; Ogawa, K.; Ukigaya, T. Sustained-release medicinal composition, 71-162657 3773920, 19710714, **1973**.
(45) Koppel, D. E. *J. Chem. Phys.* **1972**, *57* (11), 4814–4820.
(46) Ma, Q.; Wooley, K. L. *J. Polym. Sci., Part A: Polym. Chem.* **2000**, *38* (S1), 4805–4820.
(47) Huang, H.; Kowalewski, T.; Remsen, E. E.; Gertzmann, R.; Wooley, K. L. *J. Am. Chem. Soc.* **1997**, *119* (48), 11653–11659.
(48) Thompson, K.; Michielsen, S. *J. Polym. Sci., Part A: Polym. Chem.* **2005**, *44*, 126–136.
(49) Zhu, L.; Feng, S. *Chemosphere* **2003**, *53* (5), 459–467.

MA702681U